Optical and transport properties in a doped two-leg ladder antiferromagnet

Jihong Qin and Yun Song
Department of Physics, Beijing Normal University, Beijing 100875, China

Shiping Feng
Department of Physics, Beijing Normal University, Beijing 100875, China;
The Key Laboratory of Beam Technology and Material Modification of Ministry of Education, Beijing Normal University, Beijing 100875, China;
and National Laboratory of Superconductivity, Academia Sinica, Beijing 100080, China

Wei Yeu Chen
Department of Physics, Tamkang University, Tamsui 25137, Taiwan

(Received 26 September 2001; revised manuscript received 3 December 2001; published 5 April 2002)

Within the *t-J* model, the optical and transport properties of the doped two-leg ladder antiferromagnet are studied based on the fermion-spin theory. It is shown that the optical and transport properties of the doped two-leg ladder antiferromagnet are mainly governed by holon scattering. The low-energy peak in the optical conductivity is located at a finite energy, while the resistivity exhibits a crossover from the high-temperature metalliclike behavior to the low-temperature insulatinglike behavior, which is consistent with the experiments.

DOI: 10.1103/PhysRevB.65.155117 PACS number(s): 71.27.+a, 74.20.Mn, 72.10.−d

The undoped cuprate superconductors are typical Mott insulators with the antiferromagnetic long-range order (AFLRO).[1] A small amount of carrier doping to this Mott insulating state drives the metal-insulator transition and directly results in a superconducting transition at low temperatures for low carrier dopings. In the underdoped and optimally doped regimes, the normal state above the superconducting transition temperature shows many unusual properties in the sense that they do not fit in the conventional Fermi-liquid theory, and these unusual normal-state properties of the cuprate superconductors are closely related to the special microscopic conditions, i.e., Cu ions situated in a *square-planar* arrangement and bridged by oxygen ions, weak coupling between neighboring layers, and doping in such a way that the Fermi level lies near the middle of the Cu-O σ^* bond.[1,2] One common feature of these cuprate compounds is the square-planar Cu arrangement.[1,2] It is believed that the two-dimensional anisotropy is prominent in cuprate superconductors due to the layered perovskite structure, and strong quantum fluctuations with the suppression of AFLRO are key aspects.[1,2] However, it has been reported recently that some copper oxide materials, such as $Sr_{14}Cu_{24}O_{41}$, do not contain CuO_2 planes common to cuprate superconductors but consist of two-leg Cu_2O_3 ladders and edge-sharing CuO_2 chains.[3,4] Moreover, the isovalent substitution of Ca for Sr increases the hole density on the ladders by a transfer of preexisting holes in the charge reservoir layers composed of CuO_2 chains, and then the two-leg ladder copper oxide material $Sr_{14-x}Ca_xCu_{24}O_{41}$ is a superconductor under pressure.[5] Moreover, the experimental data show that the normal state is far from the standard Fermi-liquid behavior.[4,6] The neutron-scattering and muon-spin-resonance measurements on the compound $Sr_{14}Cu_{24}O_{41}$ indicate that the system is an antiferromagnet with a short-range spin order,[4,7] while the transport measurements on the material $Sr_{14-x}Ca_xCu_{24}O_{41}$ show that the behavior of the temperature-dependent resistivity is characterized by a crossover from the high-temperature metalliclike behavior to the low-temperature insulatinglike behavior,[5,6] which may be in common with those of the heavily underdoped cuprate superconducting materials.[1,2,8] Further, it has been shown[5,6] from experiments that the ratio of the interladder to in-ladder resistivities is $R=\rho_a(T)/\rho_c(T)\sim 10$. This large magnitude of the resistivity anisotropy reflects that the interladder mean free path is shorter than the interladder distance and the carriers are tightly confined to the ladders, and is also the evidence of incoherent transport in the interladder direction; therefore the common two-leg ladders in the ladder materials clearly dominate the most normal-state properties. These ladder copper oxide materials are also natural extensions of the Cu-O chain compounds towards the CuO_2 sheet structures. Other two-leg ladder compounds have also been found,[9,4] e.g., experiments suggest the realization of the two-leg ladder spin-$\frac{1}{2}$ antiferromagnet in $(VO)_2P_2O_7$. On the theoretical side, the two-leg ladder antiferromagnet may, therefore, be regarded as the realization of a unique, coherent resonating valence bond spin liquid, which may play a crucial role in the superconductivity of cuprate superconductors as emphasized by Anderson.[10] Therefore it is very important to investigate the normal-state properties of the doped two-leg ladder system using a systematic approach since it may provide deeper insights into the still not fully understood anomalous normal state of cuprate superconductors.

Many researchers have argued successfully that the *t-J* model, acting on the Hilbert space with no doubly occupied site, provides a consistent description of the physical properties of the doped antiferromagnet.[10,11] Within the *t-J* model, the normal-state properties of cuprate superconductors have been studied,[2,12,13] and the results show that the unusual normal-state properties of cuprate superconductors are caused by the strong electron correlation. Since the strong electron correlation is common for both cuprate supercon-

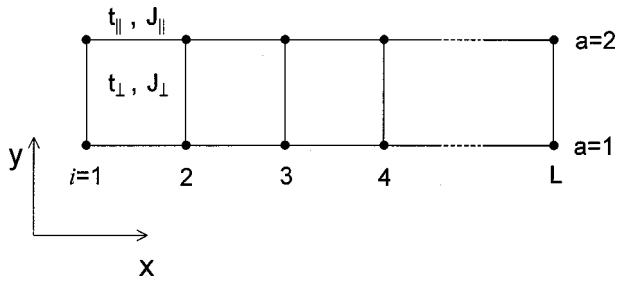

FIG. 1. The t-J ladder with two legs and L rungs. The couplings along the legs are $t_\parallel$ and $J_\parallel$, and those along the rungs $t_\perp$ and $J_\perp$.

ductors and the doped two-leg ladder antiferromagnet, the unconventional normal-state properties of the doped two-leg ladder antiferromagnet may be similar to those of the cuprate superconductors. In this paper, we study the optical and transport properties of the doped two-leg ladder antiferromagnet within the t-J model. Our results show that the low-energy peak in the optical conductivity is located at a finite energy ($\omega\sim 0.2t$), while the resistivity exhibits a crossover from the high-temperature metalliclike behavior to the low-temperature insulatinglike behavior.

The basic element of the two-leg ladder materials is the two-leg ladder, which is defined as two parallel chains of ions, with bonds among them such that the interchain coupling is comparable in strength to the couplings along the chains, while the coupling between the two chains that participate in this structure is through rungs.[4] In this case, the t-J model on the two-leg ladder is expressed as

$$H=-t_\parallel\sum_{i\hat{\eta}a\sigma} C^\dagger_{ia\sigma}C_{i+\hat{\eta}a\sigma}-t_\perp\sum_{i\sigma}\ (C^\dagger_{i1\sigma}C_{i2\sigma}+\text{H.c.})$$
$$-\mu\sum_{ia\sigma}\ C^\dagger_{ia\sigma}C_{ia\sigma}+J_\parallel\sum_{i\hat{\eta}a}\ \mathbf{S}_{ia}\cdot\mathbf{S}_{i+\hat{\eta}a}+J_\perp\sum_i\ \mathbf{S}_{i1}\cdot\mathbf{S}_{i2}, \tag{1}$$

where $\hat{\eta}=\pm c_0$, c_0 is the lattice constant of the two-leg ladder lattice, which is set as unity hereafter, i runs over all rungs, $\sigma(=\uparrow,\downarrow)$ and $a(=1,2)$ are spin and leg indices, respectively, $C^\dagger_{ia\sigma}$ ($C_{ia\sigma}$) are the electron creation (annihilation) operators, $\mathbf{S}_{ia}=C^\dagger_{ia}\vec{\sigma}C_{ia}/2$ are the spin operators with $\vec{\sigma}=(\sigma_x,\sigma_y,\sigma_z)$ being the Pauli matrices, and μ is the chemical potential. This t-J model is supplemented by the on-site single occupancy local constraint $\Sigma_\sigma C^\dagger_{ia\sigma}C_{ia\sigma}\leqslant 1$. The two-leg ladder with c and a axes parallel to ladders and rungs, respectively, is sketched in Fig. 1. In the materials of interest, the exchange coupling $J_\parallel$ along the legs is nearly the same as the exchange coupling $J_\perp$ across a rung, and similarly the hopping $t_\parallel$ along the legs is close to the rung hopping strength $t_\perp$; therefore, in the following discussions, we will work with the isotropic system $J_\perp=J_\parallel=J$, $t_\perp=t_\parallel=t$.

In the t-J model, the strong electron correlation is reflected by the local constraint. To incorporate this local constraint, the fermion-spin theory based on the charge-spin separation, $C_{ia\uparrow}=h^\dagger_{ia}S^-_{ia}$, $C_{ia\downarrow}=h^\dagger_{ia}S^+_{ia}$, has been proposed,[14] where the spinless fermion operator h_{ia} keeps track of the charge (holon), while the pseudospin operator S_{ia} keeps track of the spin (spinon), and then the local constraint can be treated properly in analytical calculations. Within this fermion-spin representation, the low-energy behavior of the t-J model (1) can be rewritten as

$$H=t\sum_{i\hat{\eta}a}\ h^\dagger_{i+\hat{\eta}a}h_{ia}(S^+_{ia}S^-_{i+\hat{\eta}a}+S^-_{ia}S^+_{i+\hat{\eta}a})+t\sum_i\ (h^\dagger_{i1}h_{i2}$$
$$+h^\dagger_{i2}h_{i1})(S^+_{i1}S^-_{i2}+S^-_{i1}S^+_{i2})+\mu\sum_{ia}\ h^\dagger_{ia}h_{ia}$$
$$+J_{\parallel\text{eff}}\sum_{i\hat{\eta}a}\ \mathbf{S}_{ia}\cdot\mathbf{S}_{i+\hat{\eta}a}+J_{\perp\text{eff}}\sum_i\ \mathbf{S}_{i1}\cdot\mathbf{S}_{i2}, \tag{2}$$

where $J_{\parallel\text{eff}}=J[(1-\delta)^2-\phi^2_\parallel]$, $J_{\perp\text{eff}}=J[(1-\delta)^2-\phi^2_\perp]$, the holon particle-hole order parameters $\phi_\parallel=\langle h^\dagger_{ia}h_{i+\hat{\eta}a}\rangle$, $\phi_\perp=\langle h^\dagger_{i1}h_{i2}\rangle$, δ is the hole doping concentration, and S^+_i and S^-_i are the pseudospin raising and lowering operators, respectively. Since the local constraint has been treated properly in the framework of the fermion-spin theory, the extra gauge degree of freedom related with the electron on-site local constraint under the charge-spin separation does not appear. In this case, the spin fluctuation couples only to spinons, while the charge fluctuation couples only to holons, but the strong correlation between holons and spinons is still considered through the holon's order parameters entering the spinon's propagator and the spinon's order parameters entering the holon's propagator; therefore both holons and spinons contribute to the charge dynamics. In this case, the optical and transport properties of the doped cuprates have been discussed[13] and the results are consistent with the experiments.[1,2] Following their discussions,[13] the optical conductivity of the doped two-leg ladder antiferromagnet can be expressed as

$$\sigma_c(\omega)=-\frac{\text{Im}\Pi^{(h)}(\omega)}{\omega}, \tag{3}$$

where $\Pi^{(h)}(\omega)$ is the holon current-current correlation function, which is defined as $\Pi^{(h)}(\tau-\tau')=-\langle T_\tau j^{(h)}(\tau)j^{(h)}(\tau')\rangle$, where τ and τ' are the imaginary times and T_τ is the τ order operator. Within the t-J Hamiltonian (2), the current densities of holons is obtained by the time derivation of the polarization operator using Heisenberg's equation of motion $j^{(h)}=2\chi_\parallel et\Sigma_{ai}\hat{\eta}h^\dagger_{ai+\hat{\eta}}h_{ai}+2\chi_\perp et\Sigma_i(R_{2i}-R_{1i})(h^\dagger_{2i}h_{1i}-h^\dagger_{1i}h_{2i})$, where R_{1i} and R_{2i} are lattice sites of leg 1 and leg 2, respectively, the spinon correlation functions $\chi_\parallel=\langle S^+_{ai}S^-_{ai+\hat{\eta}}\rangle$, $\chi_\perp=\langle S^+_{1i}S^-_{2i}\rangle$, and e is the electronic charge, which is set as unity hereafter. This holon current-current correlation function can be calculated in terms of the holon Green's function $g(k,\omega)$. However, in the two-leg ladder system, because there are two coupled t-J chains, the energy spectrum has two branches. In this case, the one-particle holon Green's function is the matrix, and can be expressed as $g(i-j,\tau-\tau')=g_L(i-j,\tau-\tau')+\sigma_x g_T(i-j,\tau-\tau')$, where the longitudinal and transverse parts are defined as $g_L(i-j,\tau-\tau')=-\langle T_\tau h_{ai}(\tau)h^\dagger_{aj}(\tau')\rangle$ and $g_T(i$

$-j,\tau-\tau')=-\langle T_\tau h_{ai}(\tau)h^\dagger_{a'j}(\tau')\rangle$ $(a\neq a')$, respectively. Then after a straightforward calculation,[13] we obtain the optical conductivity of the doped two-leg ladder antiferromagnet as

$$\sigma_c(\omega)=\sigma_c^{(L)}(\omega)+\sigma_c^{(T)}(\omega), \tag{4}$$

with the longitudinal and transverse parts are given by

$$\sigma_c^{(L)}(\omega)=4t^2\frac{1}{L}\sum_k\ (4\chi_\parallel^2\sin^2k+\chi_\perp^2)\int_{-\infty}^{\infty}\frac{d\omega'}{2\pi}A_L^{(h)}(k,\omega'+\omega)A_L^{(h)}(k,\omega')\frac{n_F(\omega'+\omega)-n_F(\omega')}{\omega}, \tag{5a}$$

$$\sigma_c^{(T)}(\omega)=4t^2\frac{1}{L}\sum_k\ (4\chi_\parallel^2\sin^2k-\chi_\perp^2)\int_{-\infty}^{\infty}\frac{d\omega'}{2\pi}A_T^{(h)}(k,\omega'+\omega)A_T^{(h)}(k,\omega')\frac{n_F(\omega'+\omega)-n_F(\omega')}{\omega}, \tag{5b}$$

respectively, where L is the number of rungs, $n_F(\omega)$ is the fermion distribution function. The longitudinal and transverse holon spectral functions $A_L^{(h)}(k,\omega)$ and $A_T^{(h)}(k,\omega)$ are obtained as $A_L^{(h)}(k,\omega)=-2\mathrm{Im}g_L(k,\omega)$ and $A_T^{(h)}(k,\omega)=-2\mathrm{Im}g_T(k,\omega)$, respectively, the full holon Green's function $g^{-1}(k,\omega)=g^{(0)-1}(k,\omega)-\Sigma^{(h)}(k,\omega)$ with the longitudinal and transverse mean-field holon Green's function $g_L^{(0)}(k,\omega)=1/2\Sigma_\nu 1/(\omega-\xi_k^{(\nu)})$ and $g_T^{(0)}(k,\omega)=1/2\Sigma_\nu(-1)^{\nu+1}1/(\omega-\xi_k^{(\nu)})$, where $\nu=1,2$, while the longitudinal and transverse second-order holon self-energy from the spinon pair bubble are obtained by the loop expansion to the second order[13] as

$$\Sigma_L(k,\omega)=\left(\frac{t}{N}\right)^2\sum_{pq}\sum_{\nu\nu'\nu''}\Xi_{\nu\nu'\nu''}(k,p,q,\omega), \tag{6}$$

$$\Sigma_T(k,\omega)=\left(\frac{t}{N}\right)^2\sum_{pq}\sum_{\nu\nu'\nu''}(-1)^{\nu+\nu'+\nu''+1}\Xi_{\nu\nu'\nu''}(k,p,q,\omega), \tag{7}$$

respectively, with $\Xi_{\nu\nu'\nu''}(k,p,q,\omega)$ given by

$$\Xi_{\nu\nu'\nu''}(k,p,q,\omega)=\frac{B_{q+p}^{(\nu')}B_q^{(\nu)}}{32\omega_{q+p}^{(\nu')}\omega_q^{(\nu)}}\{2[\gamma_{q+p+k}+\gamma_{q-k}]+[(-1)^{\nu+\nu''}+(-1)^{\nu'+\nu''}]\}^2\times\left(\frac{F^{(1)}_{\nu\nu'\nu''}(k,p,q)}{\omega+\omega_{q+p}^{(\nu')}-\omega_q^{(\nu)}-\xi_{p+k}^{(\nu'')}}+\frac{F^{(2)}_{\nu\nu'\nu''}(k,p,q)}{\omega-\omega_{q+p}^{(\nu')}+\omega_q^{(\nu)}-\xi_{p+k}^{(\nu'')}}+\frac{F^{(3)}_{\nu\nu'\nu''}(k,p,q)}{\omega+\omega_{q+p}^{(\nu')}+\omega_q^{(\nu)}-\xi_{p+k}^{(\nu'')}}+\frac{F^{(4)}_{\nu\nu'\nu''}(k,p,q)}{\omega-\omega_{q+p}^{(\nu')}-\omega_q^{(\nu)}-\xi_{p+k}^{(\nu'')}}\right), \tag{8}$$

where $\gamma_k=\cos k$, $\lambda=4J_{\parallel\mathrm{eff}}$, $\epsilon_\parallel=1+2t\phi_\parallel/J_{\parallel\mathrm{eff}}$, $\epsilon_\perp=1+4t\phi_\perp/J_{\perp\mathrm{eff}}$, and

$$B_k^{(\nu)}=B_k-J_{\perp\mathrm{eff}}[\chi_\perp+2\chi_\perp^z(-1)^\nu][\epsilon_\perp+(-1)^\nu], \tag{9a}$$

$$B_k=\lambda[(2\epsilon_\parallel\chi_\parallel^z+\chi_\parallel)\gamma_k-(\epsilon_\parallel\chi_\parallel+2\chi_\parallel^z)], \tag{9b}$$

$$F^{(1)}_{\nu\nu'\nu''}(k,p,q)=n_F(\xi_{p+k}^{(\nu'')})[n_B(\omega_q^{(\nu)})-n_B(\omega_{q+p}^{(\nu')})]+n_B(\omega_{q+p}^{(\nu')})[1+n_B(\omega_q^{(\nu)})], \tag{9c}$$

$$F^{(2)}_{\nu\nu'\nu''}(k,p,q)=n_F(\xi_{p+k}^{(\nu'')})[n_B(\omega_{q+p}^{(\nu')})-n_B(\omega_q^{(\nu)})]+n_B(\omega_q^{(\nu)})\times[1+n_B(\omega_{q+p}^{(\nu')})], \tag{9d}$$

$$F^{(3)}_{\nu\nu'\nu''}(k,p,q)=n_F(\xi_{p+k}^{(\nu'')})[1+n_B(\omega_{q+p}^{(\nu')})+n_B(\omega_q^{(\nu)})]+n_B(\omega_q^{(\nu)})n_B(\omega_{q+p}^{(\nu')}), \tag{9e}$$

$$F^{(4)}_{\nu\nu'\nu''}(k,p,q)=[1+n_B(\omega_q^{(\nu)})][1+n_B(\omega_{q+p}^{(\nu')})]-n_F(\xi_{p+k}^{(\nu'')})\times[1+n_B(\omega_{q+p}^{(\nu')})+n_B(\omega_q^{(\nu)})], \tag{9f}$$

where $n_B(\omega_k^{(\nu)})$ is the boson distribution functions, the mean-field (MF) holon excitations $\xi_k^{(\nu)}=4t\chi_\parallel\gamma_k+\mu+2\chi_\perp t(-1)^{\nu+1}$, and the MF spinon excitations

$$\begin{aligned}\omega_k^{(\nu)2}=&\alpha\epsilon_\parallel\lambda^2\left(\frac{1}{2}\chi_\parallel+\epsilon_\parallel\chi_\parallel^z\right)\gamma_k^2-\epsilon_\parallel\lambda^2\left[\frac{1}{2}\alpha\left(\frac{1}{2}\epsilon_\parallel\chi_\parallel+\chi_\parallel^z\right)\right.\\&\left.+\alpha\left(C_\parallel^z+\frac{1}{2}C_\parallel\right)+\frac{1}{4}(1-\alpha)\right]\gamma_k-\frac{1}{2}\alpha\epsilon_\perp\lambda J_{\perp\mathrm{eff}}(C_\perp\\&+\epsilon_\parallel\chi_\perp)\gamma_k+\alpha\lambda J_{\perp\mathrm{eff}}(-1)^{\nu+1}\left[\frac{1}{2}(\epsilon_\perp\chi_\parallel+\epsilon_\parallel\chi_\perp)\right.\\&\left.+\epsilon_\parallel\epsilon_\perp(\chi_\perp^z+\chi_\parallel^z)\right]\gamma_k-\alpha\epsilon_\parallel\lambda J_{\perp\mathrm{eff}}(C_\perp^z+\chi_\perp^z)\gamma_k\\&+\lambda^2\left[\alpha\left(C_\parallel^z+\frac{1}{2}\epsilon_\parallel^2C_\parallel\right)+\frac{1}{8}(1-\alpha)(1+\epsilon_\parallel^2)\right.\\&\left.-\frac{1}{2}\alpha\epsilon_\parallel\left(\frac{1}{2}\chi_\parallel+\epsilon_\parallel\chi_\parallel^z\right)\right]+\alpha\lambda J_{\perp\mathrm{eff}}[\epsilon_\parallel\epsilon_\perp C_\perp+2C_\perp^z]\\&+\frac{1}{4}J_{\perp\mathrm{eff}}^2(\epsilon_\perp^2+1)-\frac{1}{2}\epsilon_\perp J_{\perp\mathrm{eff}}^2(-1)^{\nu+1}-\alpha\lambda J_{\perp\mathrm{eff}}\\&\times(-1)^{\nu+1}\left[\frac{1}{2}\epsilon_\parallel\epsilon_\perp\chi_\parallel+\epsilon_\perp(\chi_\parallel^z+C_\perp^z)+\frac{1}{2}\epsilon_\parallel C_\perp\right],\end{aligned} \tag{10}$$

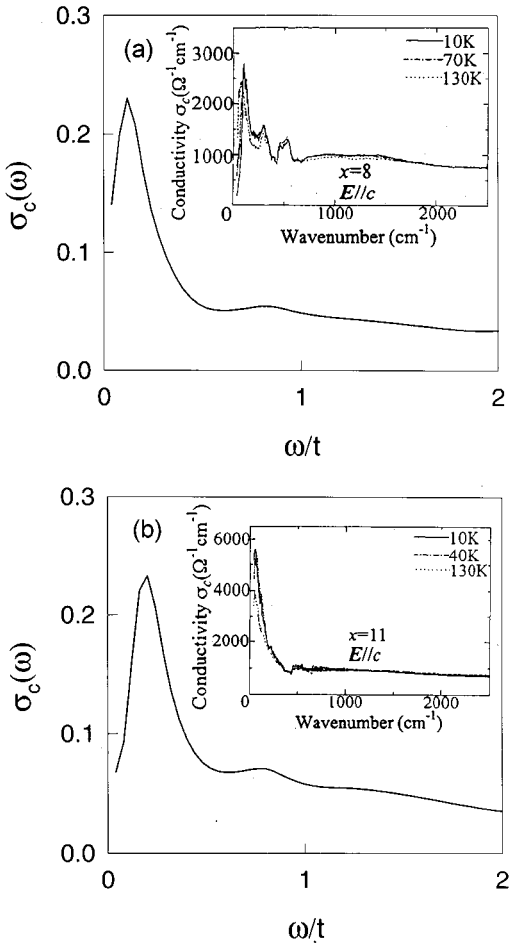

FIG. 2. The optical conductivity of the doped two-leg ladder antiferromagnet at doping (a) $\delta=0.16$ and (b) $\delta=0.20$ for parameter $t/J=2.5$ at temperature $T=0$. Inset: the experimental result on $Sr_{14-x}Ca_xCu_{24}O_{41}$ taken from Ref. 6.

with the spinon correlation functions $\chi_{\parallel}^{z}=\langle S_{ai}^{z}S_{ai+\hat{\eta}}^{z}\rangle$, $\chi_{\perp}^{z}=\langle S_{1i}^{z}S_{2i}^{z}\rangle$, $C_{\parallel}=(1/4)\Sigma_{\hat{\eta}\hat{\eta}'}\langle S_{ai+\hat{\eta}}^{+}S_{ai+\hat{\eta}'}^{-}\rangle$, and $C_{\parallel}^{z}=(1/4)\Sigma_{\hat{\eta}\hat{\eta}'}\langle S_{ai+\hat{\eta}}^{z}S_{ai+\hat{\eta}'}^{z}\rangle$, $C_{\perp}=(1/2)\Sigma_{\hat{\eta}}\langle S_{2i}^{+}S_{1i+\hat{\eta}}^{-}\rangle$, and $C_{\perp}^{z}=(1/2)\Sigma_{\hat{\eta}}\langle S_{1i}^{z}S_{2i+\hat{\eta}}^{z}\rangle$. In order not to violate the sum rule of the correlation function $\langle S_{ai}^{+}S_{ai}^{-}\rangle=1/2$ in the case without AFLRO, the important decoupling parameter α has been introduced in the mean-field calculation, which can be regarded as the vertex correction.[15] All the above mean-field order parameters have been determined by the self-consistent calculation.[15]

Now we discuss the optical and transport properties of the doped two-leg ladder antiferromagnet. The optical conductivity of the doped Mott insulator, in principle, consists of three different parts: (1) the Drude absorption, (2) absorption across the Mott-Hubbard gap, which rapidly decreases in intensity upon doping, and (3) an absorption continuum within the gap, which reflects the strong coupling between charge carriers and spin excitations. In Fig. 2, we plot the optical conductivity $\sigma_c(\omega)$ at doping (a) $\delta=0.16$ and (b) $\delta=0.20$ for parameter $t/J=2.5$ at temperature $T=0$, in comparison with the corresponding experimental data[6] taken on

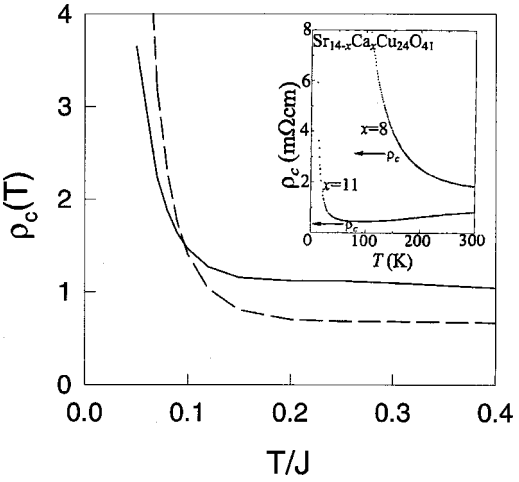

FIG. 3. The resistivity of the doped two-leg ladder antiferromagnet at doping $\delta=0.16$ (solid line) and $\delta=0.20$ (dashed line) for parameter $t/J=2.5$. Inset: the experimental result on $Sr_{14-x}Ca_xCu_{24}O_{41}$ taken from Ref. 6.

$Sr_{14-x}Ca_xCu_{24}O_{41}$ (inset), where the hole density on the ladders at $x=8$ and $x=11$ is $\delta=0.16$ and $\delta=0.20$ per Cu ladder, respectively. From Fig. 2, we find that the optical conductivity consists of two bands separated at $\omega\sim0.5t$: the higher-energy band, corresponding to the midinfrared band, shows a weak peak at $\omega\sim0.8t$ unlike a Drude peak, which dominates in the conductivity spectrum of the doped cuprate superconductors, the lower-energy peak in the present ladder systems is located at a finite energy $\omega\sim0.2t$, while the extremely small continuum absorption is consistent with the notion of the charge-spin separation. These behaviors are in agreement with the experimental results of the doped two-leg ladder antiferromagnet.[5,6] In the above calculations, we also find that the optical conductivity $\sigma_c(\omega)$ of the doped two-leg ladder antiferromagnet is essentially determined by its longitudinal part $\sigma_c^{(L)}(\omega)$, this is why in the present ladder systems the midinfrared band is much weaker than the low-energy band, and the conductivity spectrum appears to reflect the one-dimensional nature of the electronic state.[16] This conductivity of the doped two-leg ladder antiferromagnet has been discussed by Kim[17] based on a model of hole pairs forming a strongly correlated liquid, where quantum interference effects are handled using renormalization-group methods, and then the main low-energy features of the experiments are reproduced. Our results in low energy are also consistent with his results.

With the help of the optical conductivity (4), the resistivity can be obtained as $\rho_c=1/\lim_{\omega\to0}\sigma_c(\omega)$. The result of ρ_c at doping $\delta=0.16$ (solid line) and $\delta=0.20$ (dashed line) for parameter $t/J=2.5$ is shown in Fig. 3, in comparison with the corresponding experimental results[6] taken on $Sr_{14-x}Ca_xCu_{24}O_{41}$ (inset). Our results show that the behavior of the temperature dependence of $\rho_c(T)$ exhibits a crossover from the high-temperature metalliclike behavior to the low-temperature insulatinglike behavior, but the metalliclike temperature dependence dominates over a wide temperature

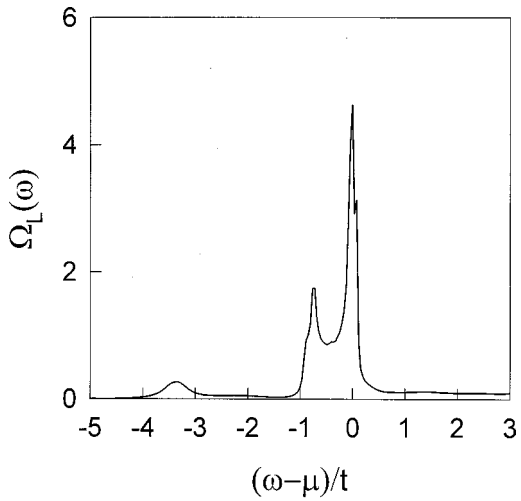

FIG. 4. The holon density of states at doping $\delta=0.16$ for parameter $t/J=2.5$ at temperature $T=0$.

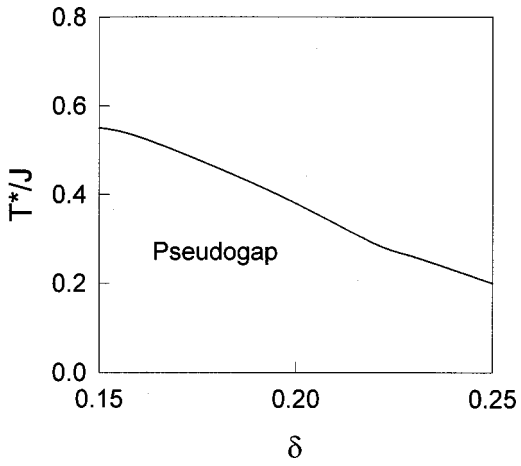

FIG. 5. The normal-state phase diagram $T^*\sim\delta$ for parameter $t/J=2.5$. T^* marks the development of the holon pseudogap in the holon density of states.

range, in agreement with the corresponding experimental data.[5,6] The present result also indicates that the behaviors of $\rho_c(T)$ in the doped two-leg ladder antiferromagnet are very similar to those of the heavily underdoped cuprate superconducting materials[1,2,8] perhaps since both materials have almost same microscopic energy scales and owing to the common corner-sharing CuO_4 networks.

In the above discussions, the central concern of the optical and transport properties in the doped two-leg ladder antiferromagnet is the quasi-one-dimensionality of the electron state, then the optical and transport properties are mainly determined by the longitudinal charged holon fluctuation. Our present study also indicates that the observed crossovers of ρ_c for the doped two-leg ladder antiferromagnet seem to be connected with the pseudogap in the charged holon excitations, which can be understood from the physical property of the holon density of states (DOS) $\Omega_L(\omega)=1/N\Sigma_k A_L^{(h)}(k,\omega)$. This holon DOS has been calculated, and the result at doping $\delta=0.16$ for parameter $t/J=2.5$ with temperature $T=0$ is plotted in Fig. 4. We therefore find that the holon DOS consists of a U-shape pseudogap near the chemical potential μ. For a better understanding of the property of this U-shape pseudogap, we plot the phase diagram $T^*\sim\delta$ at parameter $t/J=2.5$ in Fig. 5, where T^* marks the development of the pseudogap in the holon DOS. As seen from Fig. 5, this pseudogap is doping and temperature dependent and grows monotonical as the doping δ decreases and disappears at higher doping. Moreover, this pseudogap decreases with increasing temperatures and vanishes at higher temperatures. Since the full holon Green's function (then the holon spectral function and DOS) is obtained by considering the second-order correction due to the spinon pair bubble, the holon pseudogap is closely related to the spinon fluctuation. This holon pseudogap would reduce the holon scattering and thus is responsible for the metallic to insulating crossover in the resistivity ρ_c. While in the region where the holon pseudogap closes at high temperatures, the charged holon scattering would give rise to the metallic temperature dependence of the resistivity.

In summary, we have studied the optical and transport properties of the doped two-leg ladder antiferromagnet within the t-J model. Our result shows that the optical and transport properties of the doped two-leg ladder antiferromagnet are mainly governed by the charged holon scattering. The low-energy peak in the optical conductivity is located at a finite energy, while the resistivity exhibits a crossover from the high-temperature metalliclike behavior to the low-temperature insulatinglike behavior, in agreement with the experiments.

Finally, we emphasize that in the above discussions, only the results of the doped isotropic two-leg ladder system are presented. However, we[18] have also studied the physical properties of the anisotropic system, i.e., $J_\perp<J_\parallel$ and $t_\perp<t_\parallel$. In this case, the interference effects between the two legs are decreased by decreasing the values of $J_\perp/J_\parallel$ and $t_\perp/t_\parallel$; this leads to the low-energy peak of the conductivity being located at $\omega\sim0$ instead of a finite energy for the isotropic system. On the other hand, it has been shown that the interleg single-electron hopping changes the asymptotic behavior of the interleg spin-spin correlation functions, but their exponents are independent of the interleg coupling strength.[19] We believe that the evolution of the incommensurate magnetic fluctuations with dopings in the doped square lattice antiferromagnet[20] will also occur in the doped two-leg antiferromagnet, and the related theoretical results will be presented elsewhere.

ACKNOWLEDGMENTS

The authors would like to thank Dr. Feng Yuan and Xianglin Ke for helpful discussions. This work was supported by the National Natural Science Foundation for Distinguished Young Scholars under Grant No. 10125415, the National Natural Science Foundation under Grants Nos. 10074007 and 90103024, a Grant from the Ministry of Education of China, and the National Science Council under Grant No. NSC 90-2816-M-032-0001-6.

[1] M.A. Kastner, R.J. Birgeneau, G. Shiran, and Y. Endoh, Rev. Mod. Phys. **70**, 897 (1998); A.P. Kampf, Phys. Rep. **249**, 219 (1994).

[2] See, e. g., *Proceedings of Los Alamos Symposium*, edited by K. S. Bedell, D. Coffey, D. E. Meltzer, D. Pines, and J. R. Schrieffer (Addison-Wesley, Redwood City, CA, 1990); P. W. Anderson, *The Theory of Superconductivity in the High-T_c Cuprates* (Princeton University Press, Princeton, NJ, 1997).

[3] M. Azuma, Z. Hiroi, M. Takano, K. Ishida, and Y. Kitaoka, Phys. Rev. Lett. **73**, 3463 (1994).

[4] E. Dagotto and T.M. Rice, Science **271**, 618 (1996), and references therein.

[5] T. Nagata, M. Uehara, J. Goto, J. Akimitsu, N. Motoyama, H. Eisaki, S. Uchida, H. Takahashi, T. Nakanishi, and N. Mori, Phys. Rev. Lett. **81**, 1090 (1998); M. Uehara, T. Nagata, J. Akimitsu, H. Takahashi, N. Mori, and K.K. Kinoshita, J. Phys. Soc. Jpn. **65**, 2764 (1996).

[6] T. Osafune, N. Motoyama, H. Eisaki, S. Uchida, and S. Tajima, Phys. Rev. Lett. **82**, 1313 (1999); T. Osafune, N. Motoyama, H. Eisaki, and S. Uchida, *ibid.* **78**, 1980 (1997).

[7] T. Imai, K.R. Thurber, K.M. Shen, A.W. Hunt, and F.C. Chou, Phys. Rev. Lett. **81**, 220 (1998); Y. Sidis, M. Braden, P. Bourges, B. Hennion, S. NishiZaki, Y. Maeno, and Y. Mori, *ibid.* **83**, 3320 (1999).

[8] H. Takagi, B. Batlogg, H.L. Kao, J. Kwo, R.J. Cava, J.J. Krajewski, and W.F. Peck, Phys. Rev. Lett. **69**, 2975 (1992).

[9] D.C. Johnston, J.W. Johnson, D.P. Goshom, and A.P. Jacobson, Phys. Rev. B **35**, 219 (1987).

[10] P. W. Anderson, in *Frontiers and Borderlines in Many Particle Physics*, edited by R. A. Broglia and J. R. Schrieffer (North-Holland, Amsterdam, 1987), P. 1; Science **235**, 1196 (1987).

[11] F.C. Zhang and T.M. Rice, Phys. Rev. B **37**, 3759 (1988); T.M. Rice, Physica C **282-287**, xix (1997).

[12] E. Dagotto, Rev. Mod. Phys. **66**, 763 (1994), and references therein.

[13] Shiping Feng and Zhongbing Huang, Phys. Lett. A **232**, 293 (1997); Phys. Rev. B **57**, 10 328 (1998).

[14] Shiping Feng, Z.B. Su, and L. Yu, Phys. Rev. B **49**, 2368 (1994); Mod. Phys. Lett. B **7**, 1013 (1993).

[15] J. Kondo and K. Yamaji, Prog. Theor. Phys. **47**, 807 (1972); Shiping Feng and Yun Song, Phys. Rev. B **55**, 642 (1997).

[16] P. Horsch and W. Stephan, Phys. Rev. B **48**, 10 595 (1993).

[17] E.H. Kim, Phys. Rev. Lett. **86**, 1315 (2001).

[18] Jihong Qin, Ying Huang, and Shiping Feng (unpublished).

[19] G.M. Zhang, Shiping Feng, and Lu Yu, Phys. Rev. B **49**, 9997 (1994).

[20] K. Yamada, C.H. Lee, K. Kurahashi, J. Wada, S. Wakimoto, S. Ueki, H. Kimura, Y. Endoh, S. Hosoya, and G. Shirane, Phys. Rev. B **57**, 6165 (1998); P. Dai, H.A. Mook, R.D. Hunt, and F. Doğan, *ibid.* **63**, 054525 (2001); Feng Yuan, Shiping Feng, Zhao-Bin Su, and Lu Yu, *ibid.* **64**, 224505 (2001).